Glycobiology vol. 21 no. 1 pp. 82–98, 2011
doi:10.1093/glycob/cwq134
Advance Access publication on September 20, 2010

High-sensitivity *O*-glycomic analysis of mice deficient in core 2 β1,6-*N*-acetylglucosaminyltransferases

Mohd Nazri Ismail[2], Erica L Stone[3], Maria Panico[2], Seung Ho Lee[4], Ying Luu[5], Kevin Ramirez[3], Samuel B Ho[5], Minoru Fukuda[4], Jamey D Marth[6], Stuart M Haslam[2], and Anne Dell[1,2]

[2]Division of Molecular Biosciences, Faculty of Natural Sciences, Imperial College London, London SW7 2AZ, UK; [3]Department of Cellular and Molecular Medicine, University of California-San Diego, La Jolla, CA 92093, USA; [4]Burnham Institute for Medical Research, La Jolla, CA 92037, USA; [5]Department of Medicine, VA San Diego Healthcare System and the University of California, San Diego, CA 92161, USA; and [6]Center for Nanomedicine, Sanford-Burnham Medical Research Institute, University of California-Santa Barbara, 2324 Life Sciences Building-9625, Santa Barbara, CA 93106-9625, USA

Received on July 16, 2010; revised on August 25, 2010; accepted on August 26, 2010

Core 2 β1,6-*N*-acetylglucosaminyltransferase (C2GnT), which exists in three isoforms, C2GnT1, C2GnT2 and C2GnT3, is one of the key enzymes in the *O*-glycan biosynthetic pathway. These isoenzymes produce core 2 *O*-glycans and have been correlated with the biosynthesis of core 4 *O*-glycans and I-branches. Previously, we have reported mice with single and multiple deficiencies of C2GnT isoenzyme (s) and have evaluated the biological and structural consequences of the loss of core 2 function. We now present more comprehensive *O*-glycomic analyses of neutral and sialylated glycans expressed in the colon, small intestine, stomach, kidney, thyroid/trachea and thymus of wild-type, C2GnT2 and C2GnT3 single knockouts and the C2GnT1–3 triple knockout mice. Very high-quality data have emerged from our mass spectrometry techniques with the capability of detecting *O*-glycans up to at least 3500 Da. We were able to unambiguously elucidate the types of *O*-glycan core, branching location and residue linkages, which allowed us to exhaustively characterize structural changes in the knockout tissues. The C2GnT2 knockout mice suffered a major loss of core 2 *O*-glycans as well as glycans with I-branches on core 1 antennae especially in the stomach and the colon. In contrast, core 2 *O*-glycans still dominated the *O*-glycomic profile of most tissues in the C2GnT3 knockout mice. Analysis of the C2GnT triple knockout mice revealed a complete loss of both core 2 *O*-glycans and branched core 1 antennae, confirming that the three known isoenzymes are entirely responsible for producing these structures. Unexpectedly, *O*-linked mannosyl glycans are upregulated in the triple deficient stomach. In addition, our studies have revealed an interesting terminal structure detected on *O*-glycans of the colon tissues that is similar to the RM2 antigen from glycolipids.

Keywords: C2GnT / core 2 *O*-glycan / knockout mice / mass spectrometry / murine *O*-glycome

Introduction

Mucin-type *O*-glycans are the most commonly found *O*-glycans on secreted and membrane-associated proteins in mammalian tissues. The biosynthetic pathway of mucin-type *O*-glycans is initiated by the addition of an *N*-acetylgalactosamine (GalNAc) residue on serine or threonine (Tn antigen) by a family of UDP-GalNAc: polypeptide α-*N*-acetylgalactosaminyltransferases. The Tn antigen can then be further modified or elongated to produce up to eight core types in mammals. This biosynthetic pathway involves numerous enzymes localized in the Golgi, which contribute to the complexity and variety of *O*-glycosylation (Tian and Ten Hagen 2009).

The Tn antigen can either be sialylated or elongated via the synthesis of core 1 *O*-glycans. Core 1 *O*-glycans are initiated by the action of core 1 β1,3-galactosyltransferase on the Tn antigen. Core 1 structures are commonly either sialylated/disialylated or branched on position 6 of the GalNAc producing the core 2 *O*-glycans. The latter are biosynthesized by the enzyme core 2 β1,6-*N*-acetylglucosaminyltransferase (C2GnT), which is known to exist in three isoforms, C2GnT1, C2GnT2 and C2GnT3. Previously, we have shown that in the mouse, C2GnT2 is highly expressed mainly in the stomach and the colon, whereas C2GnT3 is highly expressed mainly in the small intestine, liver and spleen (Stone et al. 2009). On the other hand, C2GnT1 is more widely expressed in most tissues (Yeh et al. 1999).

The C2GnT gene (C2GnT1) was first cloned in 1992 (Bierhuizen 1992) and since then many efforts have been directed toward fully understanding core 2 *O*-glycans and the enzymes involved. For example, Hiraoka et al. (2004) showed that core 2 *O*-glycans, via the sialyl Lewis^x terminal antigen, are crucial for lymphocyte homing in mice. This finding was further clarified by Gauguet et al. (2004), who suggested that C2GnT1 exerts differential control over B- and T-lymphocyte

[1]To whom correspondence should be addressed: Tel: +44-2075945219; Fax: +44-2072250458; e-mail: a.dell@imperial.ac.uk

homing (Gauguet et al. 2004). Yeh et al. (1999) cloned a second C2GnT gene (C2GnT2) and proposed the idea that C2GnT2 could also be involved in synthesizing core 4 *O*-glycans and I-branches on *O*-glycans. The latter were originally thought to be solely produced by "big I" β-1,6-*N*-acetylglucosaminyltrasferase (IGnT) isoenzymes. C2GnT3, which was first cloned in 2000, has been postulated to play an important role in T-cell biology due to its relatively high expression in the human thymus (Schwientek et al. 2000). Although many functions of C2GnT have been discovered, previous studies have provided little evidence to associate their findings specifically with each of the isoenzymes and glycan structures that the isoenzymes initiated. It is also still unclear as to how much these isoenzymes compensate each other's activities.

Although oligosaccharide functions are mostly determined by terminal antigens, it has been demonstrated that their synthesis is often not regulated through terminal or intermediate glycosyltransferases, but by the branching glycosyltransferases (Ellies et al. 1998; Kikuchi et al. 2005) such as C2GnT. Therefore, it is important to investigate the correlation between C2GnT properties and the etiology of diseases.

We have previously performed phenotypic analyses on mice deficient in C2GnT2 and C2GnT3 isoenzymes (Stone et al. 2009). C2GnT2-deficient mice were found to have an impaired mucosal barrier function, augmented susceptibility to dextran sodium sulfate (DSS)-induced colitis, reduced immunoglobulin abundance and loss of core 4 biosynthetic activity. C2GnT3-deficient mice, on the other hand, had reduced the levels of circulating thyroxine and they exhibited altered behavior. We also described preliminary data from *O*-glycomic screening of tissues that indicated substantial alterations in *O*-glycan structures in some of the knockout tissues. We now report the results of in-depth mass spectrometric comparison of the neutral and sialylated *O*-glycomes of the colon, small intestine, stomach, kidney, thyroid/trachea and thymus from knockout mice and their wild-type littermates.

Even for wild-type mice, very little work has been done until now to rigorously characterize their *O*-glycosylation, despite the importance of mouse models in human biomedical research (Austin et al. 2004). Therefore, the present work also aimed to provide a more comprehensive structural characterization of the *O*-glycomes of various wild-type murine tissues.

Results

Exhaustive tandem mass spectrometric analysis of permethylated products of reductive elimination differentiates glycan isoforms and terminal epitopes

The murine tissues analyzed were the stomach, colon, small intestine and kidneys from C2GnT2 and C2GnT3 single knockouts and C2GnT1–3 triple knockout mice, plus the thymus of C2GnT3 and the thyroid/trachea of C2GnT3 and C2GnT triple knockout mice. Tissues were selected based on the expression profiles of C2GnTs supplemented by phenotypic data emerging throughout the study. The glycomic strategy employed was a refinement of earlier methodologies (Dell et al. 1994). First, tissue lysates were reduced/carboxymethylated and digested with trypsin to facilitate the subsequent release of *N*- and *O*-glycans. After PNGase F digestion of *N*-glycans, *O*-glycans were released by reductive elimination. Purified *O*-glycans were permethylated to increase the sensitivity of detection and to direct the subsequent mass spectrometric fragmentation. Consistent and reproducible data were obtained from at least two repeats of experiments.

Mass fingerprinting and sequencing were primarily carried out using a matrix-assisted laser desorption/ionization-time-of-flight (MALDI-TOF)/TOF mass spectrometer. Additional analyses using electrospray ionization (ESI)-quadrupole TOF (QTOF)-mass spectrometry (MS), MALDI-quadrupole ion trap (QIT)-TOF-MS and gas chromatography (GC)-electron impact (EI)-MS were performed on selected samples. The tandem mass spectrometric (MS/MS) analysis enabled differentiation of the structures and the sequences of glycans with the same *m/z* (mass over charge ratio) value and composition. Figure 1 shows an example of how MS/MS data were used to characterize glycan structures. The stomach of the wild-type and C2GnT2 knockout mice shared a molecular ion at *m/z* 1331 in their mass fingerprint (Figure 1A and B), and the MS/MS spectra of each of these ions are reproduced in the figure. It is evident that in the wild-type mice, the ion at *m/z* 1331 corresponds to a core 2 glycan (see annotated cartoon in Figure 1C). However, in the C2GnT2 knockout mice, the fragmentation was clearly different (Figure 1D). In this case, fragment ions attributable to the core 2 *O*-glycan are relatively minor and all major fragment ions are assignable to the elongated core 1 *O*-glycan shown in the annotation.Definitive fragments for the core 1 *O*-glycan are *m/z* 298, 520 and 1056. This MS/MS strategy for unambiguously differentiating between core 1 and core 2 antennae, and assigning antennae sequences, was applied to all analyses throughout this study.

Glycomic analysis of the colon from wild-type and knockout mice

The *O*-glycomic analysis of the colon from wild-type mice is presented in a simplified mass spectrum from *m/z* 1000 to 2000 in Figure 2A as well as in a full range and with detailed annotations in Supplementary data, Figure S3. All glycan structures detected, including from the knockout tissues, are collated in Table I. The results showed that the wild-type colon is dominated by core 2 *O*-glycans, e.g. at *m/z* 1024 ($HexNAc_3Hex_1$) and 1763 ($HexNAc_3Hex_2Fuc_1NeuAc_1$) (Table I). Core 1 *O*-glycans are of lower abundance, for instance, at *m/z* 1198 and 1950. I-branches on the galactose (Gal) of core 1 were also detected on both core 1 and core 2 *O*-glycans, for instance, at *m/z* 1432 ($HexNAc_3Hex_3$) and 1881 ($HexNAc_4Hex_4$), respectively. It was also evident that the colon was rich with glycans that are terminated with the Sd^a epitope, for example, at *m/z* 1140 ($HexNAc_2Hex_1NeuAc_1$) and 2196 ($HexNAc_4Hex_2NeuAc_2$), with the latter carrying two Sd^a epitopes (Table I).

C2GnT2 is highly expressed in the colon relative to other tissues (Stone et al. 2009). As expected, the deficiency of this isoenzyme caused immense structural changes (simplified mass spectrum in Figure 2B, full-range mass spectra in Supplementary data, Figure S4 and collated structures in

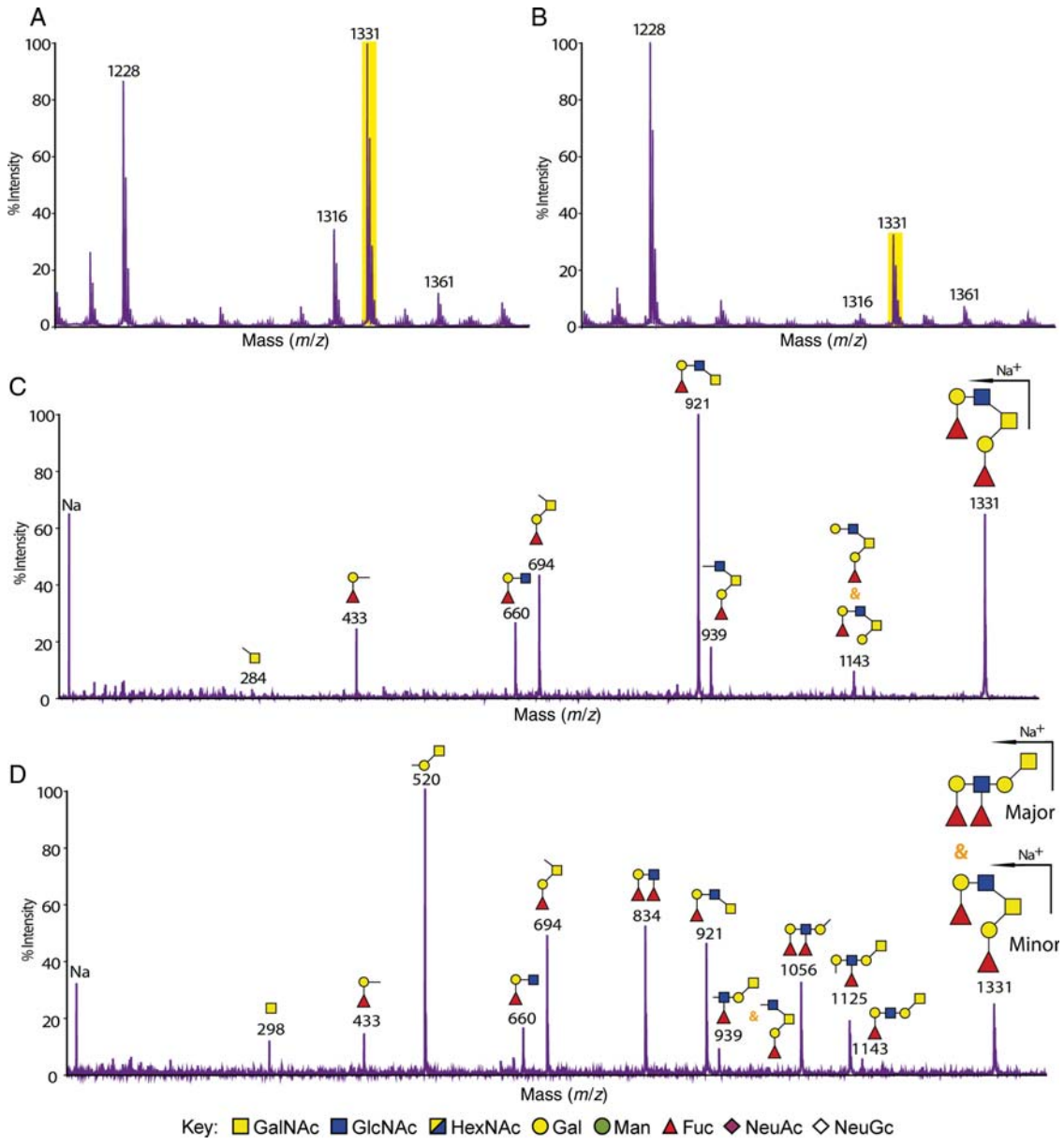

Fig. 1. MALDI-TOF/TOF-MS and MS/MS spectra of the molecular ion *m/z* 1331 $[M + Na]^+$ detected in the mass fingerprinting of the stomach from wild-type and C2GnT2 knockout mice. Selected sections from *O*-glycomic mass fingerprinting of the stomach from wild-type (**A**) and C2GnT2 knockout (**B**) mice showing several $[M + Na]^+$ peaks with the same *m/z*. High-sensitivity MS/MS data differentiate glycans of the same composition ($HexNAc_2Hex_2Fuc_2$) and mass (*m/z* 1331) but with different *O*-glycan core types. In the wild-type stomach (**C**), the core 2 *O*-glycan was the only isoform detected, whereas in the C2GnT2 knockout mice (**D**), there was a mixture of core 2 and core 1 *O*-glycans with the latter as the major component. Na, sodium.

Table I). Analysis of the colon from C2GnT2 knockout mice showed that most core 2 *O*-glycan structures have been replaced with linear core 1 structures. For example, the glycan at *m/z* 1157 ($HexNAc_2Hex_2Fuc$) in the wild-type mice was a core 2 *O*-glycan terminated with the H antigen (Table I). In the C2GnT2 knockout colon, it was revealed by MS/MS analysis that the same glycan composition was a linear core 1 *O*-glycan still terminated with the H antigen (Table I). Interestingly, there were also changes in the type of terminal epitopes consequent upon loss of the core 2 branch. For example, there was an increase in fucosylation density on individual glycan antennae leading to the formation of the atypical glycan epitope Lewis^y on the core 1 *O*-glycan at *m/z* 1331 ($HexNAc_2Hex_2Fuc_2$). The isobaric glycan in the wild-type has a core 2 structure terminated with two H antigens (Table I). In addition, there was also a reduction in glycans carrying theI-branch in the C2GnT2 knockout colon compared with the wild-type, for example, at *m/z* 1432 and 1881 (Table I).

C2GnT3 is expressed at relatively low abundance in the colon (Stone et al. 2009). As shown by the MS analysis (Figure 2C, Supplementary data, Figure S5 and Table I),

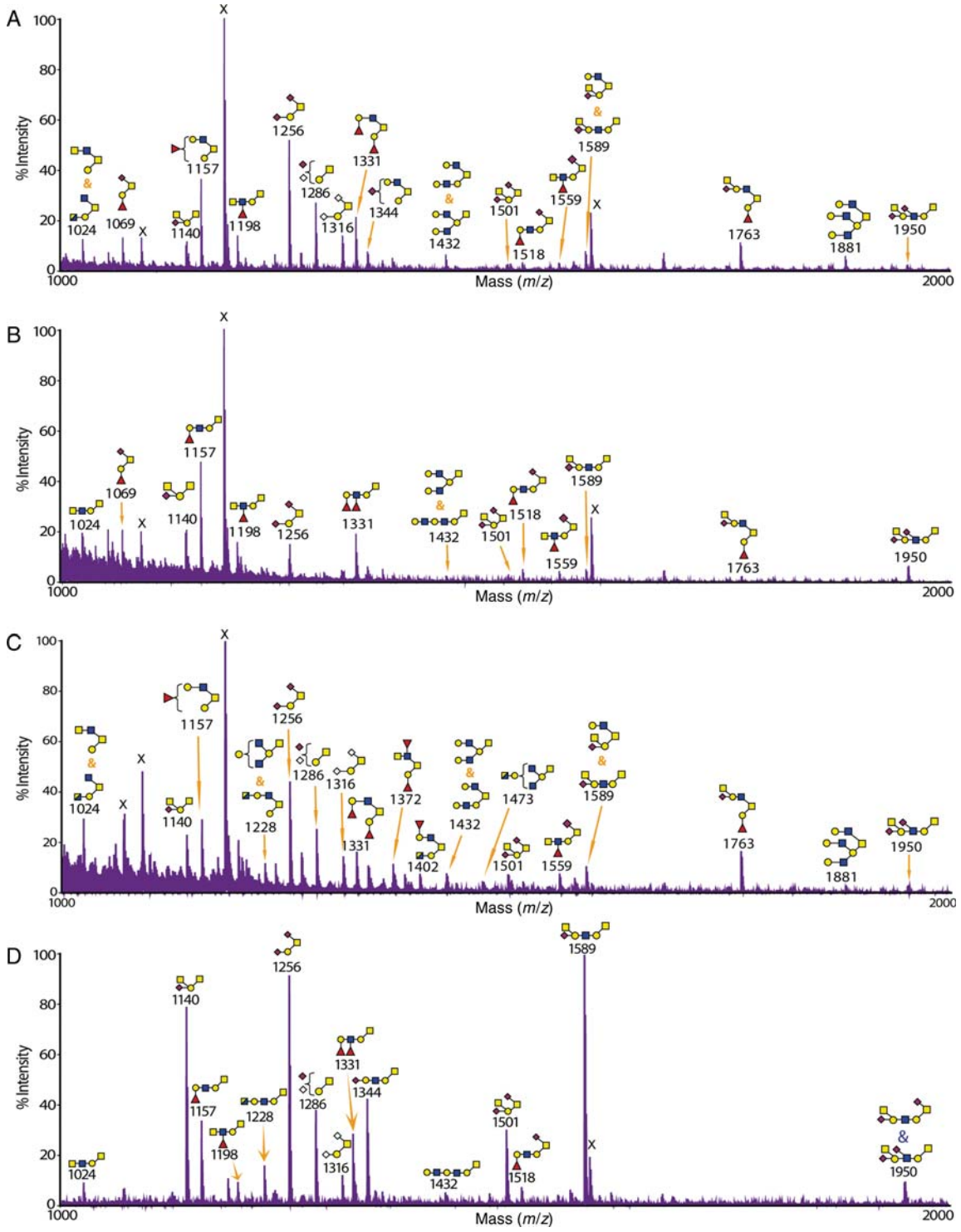

Fig. 2. MALDI-TOF-MS profile of *O*-glycans from the colon of wild-type and knockout mice. The glycomic profiles of reduced and permethylated *O*-glycans $[M + Na]^+$ detected in the colon of (**A**) wild-type, (**B**) C2GnT2 knockout, (**C**) C2GnT3 knockout and (**D**) C2GnT triple knockout mice. Cartoon structures assigned were based on mass spectrometric data and knowledge of *O*-glycan biosynthetic pathways for the selected range of *m*/*z* 1000–2000. The RM2-like antigen was detected on the glycan at *m*/*z* 1950. The full-range MALDI-TOF-MS spectra for each tissue are presented in Supplementary data, Figures S3–S6.

O-glycan structures from the colon of C2GnT3 knockout mice were quite similar to the colon of wild-type mice. For example, the glycan at *m*/*z* 1157 in the wild-type and C2GnT3 knockout tissues were both core 2 type (Table I). Another example, at *m*/*z* 1432, there was a mixture of core 1 and core 2 isoforms with the same composition in the wild type colon and the mixture remained similar in the C2GnT3 knockout (Table I).

Table I. *O*-glycan structures from the colon of wild-type and knockout mice

m/z	Structures			
	WT	C2GnT2 KO	C2GnT3 KO	C2GnT Triple KO
534				
708				
779				
895				
925		ND		
953		ND		ND
983				
1024				
1069			ND	ND
1140				
1157				
1187			ND	
1198			ND	
1228	ND	ND		
1256				
1286		ND		
1316		ND		
1331				
1344		ND	ND	
1372	ND	ND		ND

m/z	Structures			
	WT	C2GnT2 KO	C2GnT3 KO	C2GnT Triple KO
1402	ND	ND		ND
1432				
1473	ND	ND		ND
1501				
1518			ND	
1559				ND
1589				
1677	ND		ND	ND
1692	ND		ND	ND
1763				ND
1882				ND
1950				
2125		ND		ND
2196		ND		ND
2260		ND	ND	ND

Key: GalNAc GlcNAc HexNAc Gal Man Fuc NeuAc NeuGc

This table summarizes all structures $[M + Na]^+$ observed in the MALDI-TOF-MS spectra of the colon tissues from wild-type, C2GnT2 knockout, C2GnT3 knockout and C2GnT triple knockout mice. WT, wild-type mice; C2GnT2 KO, C2GnT2 knockout mice; C2GnT3 KO, C2GnT3 knockout mice; C2GnT triple KO, C2GnT triple knockout mice; ND, not detected.

The triple knockout mice lack the ability to synthesize all three known isoforms of C2GnT. This multiple deficiency caused a complete absence of core 2 *O*-glycans in the colon (Figure 2D, Supplementary data, Figure S6 and Table I). In addition, there was also a complete disappearance of I-branches on both core 1 and core 2 *O*-glycans. For example, in the wild-type colon, glycans at *m/z* 1432 consisted of core 2 and branched core 1 structures, whereas in the triple knockout colon, an elongated linear core 1 structure was detected (Table I).

Glycomic analysis of the stomach from wild-type and knockout mice

O-glycomic analysis of the stomach from wild-type mice revealed that this tissue, similar to the colon, was dominated with core 2 *O*-glycans (Figure 3A and Supplementary data, Figure S7; all structures are also summarized in Supplementary data, Table SI). One of the unique features of this tissue is the detection of high-mass *O*-glycan structures up to *m/z* 3476 (Supplementary data, Figure S7). The most abundant terminal epitope in the stomach was found to be the H antigen, for example, at *m/z* 1157 and 1331 (Figure 3A and Supplementary data, Table SI). In addition, core 1 and core 2 *O*-glycans in this tissue were found to be highly branched on the core 1 arm, similar to what was seen in the colon, for example, glycans at *m/z* 1431 and 1881. Interestingly, the glycan at *m/z* 1473 ($HexNAc_4Hex_2$), which is a core 2 *O*-glycan carrying *N*-acetylhexosamine (HexNAc)-terminated antennae, was detected at a significant level. This glycan has been postulated to carry the rare and functionally important

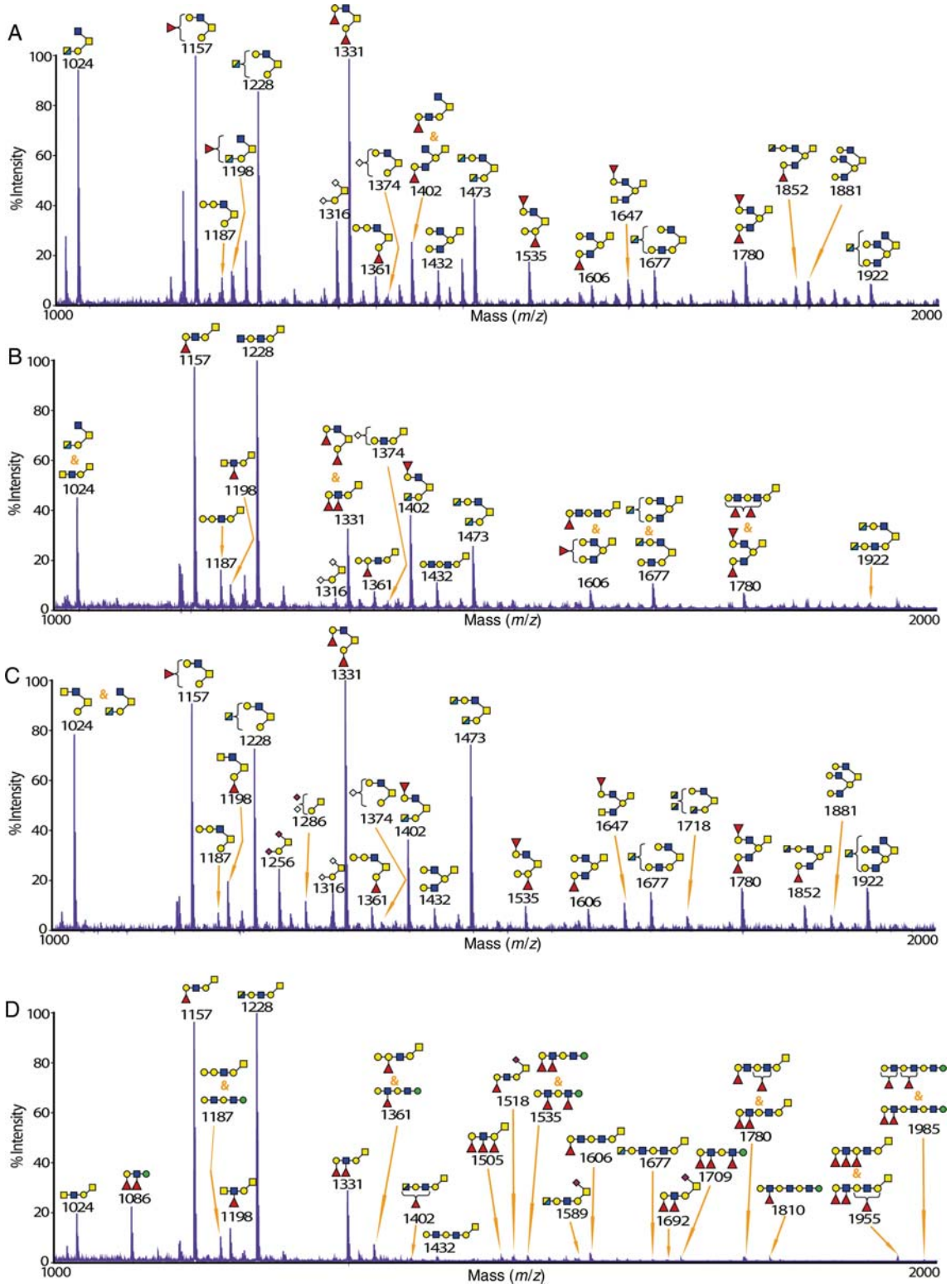

Fig. 3. MALDI-TOF-MS spectra of *O*-glycans from the stomach of wild-type and knockout mice. The glycomic profiles of reduced and permethylated *O*-glycans $[M + Na]^+$detected in the stomach of (**A**) wild-type, (**B**) C2GnT2 knockout, (**C**) C2GnT3 knockout and (**D**) C2GnT triple knockout mice. Cartoon structures assigned were based on mass spectrometric data and knowledge of *O*-glycan biosynthetic pathways for the selected range of *m*/*z* 1000–2000. The full-range MALDI-TOF-MS spectra for each tissue are presented in Supplementary data, Figures S7–S10.

N-acetylglucosamine (GlcNAc)α1-4Gal epitope that was recently identified in the wild-type mouse stomach (Kawakubo et al. 2004; Lee et al. 2008). However, enzymatic digestion with β-*N*-acetylhexosaminidase/HEXase I caused a significant reduction in this glycan showing that the terminal HexNAc residues are mainly β-linked GlcNAc.

In the C2GnT2 knockout mice, as expected, due to the relatively high expression level of C2GnT2 in the stomach (Stone et al. 2009), there was a great reduction in core 2 *O*-glycans compared with the wild-type mice (Figure 3B and Supplementary data, Figure S8 and Table SI). Glycans at *m/z* 1473, 1677 and 1922 are examples of the remaining core 2 structures, all carrying one or two terminal HexNAc residues (Figure 3B and Supplementary data, Table SII). The C2GnT2-deficient mice synthesized abundant extended core 1 *O*-glycans in the stomach, for instance, at *m/z* 1187, 1331 and 1361. Moreover, a significant reduction in branched *O*-glycans was also observed in the stomach at *m/z* 1606 and 1780. Similar to the colon of C2GnT2 knockout mice, there was an increase in fucosylation density on individual glycan antennae leading to the formation of Lewis^{y}, which was not detected in the wild-type, for instance, on the glycan at *m/z* 1331. Another interesting finding from this tissue was a minor emergence of *O*-linked mannosyl glycans at *m/z* 738 and 912, which were not detected in the wild-type stomach.

C2GnT3 is also not the main C2GnT isoenyzme in the stomach (Stone et al. 2009). There were no substantial changes in the *O*-glycomic profile of the stomach from C2GnT3 knockout mice (Figure 3C and Supplementary data, Figure S9 and Table SI). However, unexpectedly, there was an increase in the glycan at *m/z* 1473 ($HexNAc_4Hex_2$), which is a core 2 *O*-glycan carrying HexNAc-terminated antennae as seen in the wild-type and C2GnT2 knockout stomach.

In the stomach of C2GnT triple knockout mice, there was a complete loss of core 2 *O*-glycans (Figure 3D and Supplementary data, Figure S10 and Table SI). A significant reduction in nonfucosylated *O*-glycans compared with the wild-type and both single knockouts was also observed, for example, at *m/z* 1024, 1432, 1473, 1677 and 1922 in the stomach (Figure 3 and Supplementary data, Table SI). There was also an emergence of highly fucosylated and elongated *O*-linked mannose structures (for instance, at *m/z* 1187, 1535, 1709, 1810 and 1985), which were not detected at significant levels in the stomach of wild-type and C2GnT3 knockout mice and were very minor in the C2GnT2 knockout stomach (Figure 3D and Supplementary data, Table SI). The existence of *O*-linked mannose is supported by the detection of 2-linked mannitol by GC-MS linkage analysis (data not shown).

Glycomic analysis of the small intestine from wild-type and knockout mice

The *O*-glycomic analysis of small intestine from wild-type mice showed that, similar to the stomach and the colon, it was dominated by core 2 *O*-glycans, for example, at *m/z* 1402 and 1647 (Figure 4A and Supplementary data, Figure S11 and Table SII). The most abundant terminal epitopes were the H antigen (for example, on glycans at *m/z* 1157 and 1331) and Sd^{a} (for example, at *m/z* 1140 and 1589).

In contrast to the stomach and the colon, core 2 *O*-glycans were still the major structures in the small intestine of C2GnT2 knockout mice (Figure 4B and Supplementary data, Figure S12 and Table SII). There was a moderate emergence of core 1 structures whose glycan compositions were not detected in the wild-type such as *m/z* 1501 and 1950, both carrying the Sd^{a} epitope. Increase in core 1 structures sialylated with *N*-acetylneuraminic acid (NeuAc) and/or *N*-glycolylneuraminic acid (NeuGc), such as at *m/z* 1256, 1286 and 1316, was also observed. In addition, there were increases in the abundance of molecular ions whose MS/MS spectra showed that they were mixtures of core 1 and core 2 structures, for example, at *m/z* 1157 and 1589.

C2GnT3 is highly expressed in the small intestine relative to other tissues (Stone et al. 2009). The C2GnT3 deficiency in the small intestine caused a relatively moderate reduction in core 2 structures with or without an increase in their core 1 isoforms compared with the wild-type mice, for example, at *m/z* 1331 and 1589 (Figure 4C and Supplementary data, Figure S13 and Table SII). In contrast to the wild-type small intestine, there was a global reduction in glycans carrying the H antigen (for example, at *m/z* 1157 and 1402), leaving the Sd^{a} epitope as the most abundant terminal epitope, for example, at *m/z* 1140 and 1589. Similar to the C2GnT2-deficient small intestine, there were increases in sialylated core 1 structures compared with the wild-type, for instance, at *m/z* 1256, 1286 and 1316.

The small intestine of the triple knockout mice again demonstrated a complete disappearance of core 2 structures (Figure 4D and Supplementary data, Figure S14 and Table SII). Similar to the C2GnT3-deficient small intestine, the Sd^{a} epitope was the most abundant type of terminal structure, for instance, at *m/z* 1140 and 1589 (Figure 4D and Supplementary data, Table SII). Interestingly, at *m/z* 1344, it was shown by the MS/MS analysis that there was a mixture of sialylated core 1 *O*-glycans and an elongated *O*-linked mannose structure terminated with the Sd^{a} epitope. *O*-linked mannosyl glycans were not detected at any significant levels in the wild-type and single knockouts of small intestine.

Glycomic analysis of the thyroid/trachea, kidneys and thymus from wild-type and knockout mice

O-glycomic analysis of the thyroid/trachea and the kidneys from wild-type mice showed that, similar to other tissues, core 2 structures were the most abundant type of *O*-glycan (Figure 5A and Supplementary data, Figure S1A), whereas in the wild-type thymus, core 1 structures were the most abundant (Supplementary data, Figure S2A). In the thyroid/trachea, a relatively less number of glycan structures were detected and mostly were terminated with sialylation either on its own or as part of the Sd^{a} epitope, for example, at *m/z* 1344 and 1589, respectively (Figure 5A). In the wild-type kidneys, however, the core 2 *O*-glycans were moderately fucosylated leading to the formation of H- and Lewis$^{x/y}$-terminal epitopes, for example, on glycans at *m/z* 1157 and 1606 (Supplementary data, Figure S1A). In the thymus, similar to the thyroid/trachea, few *O*-glycan structures were detected (Supplementary data,

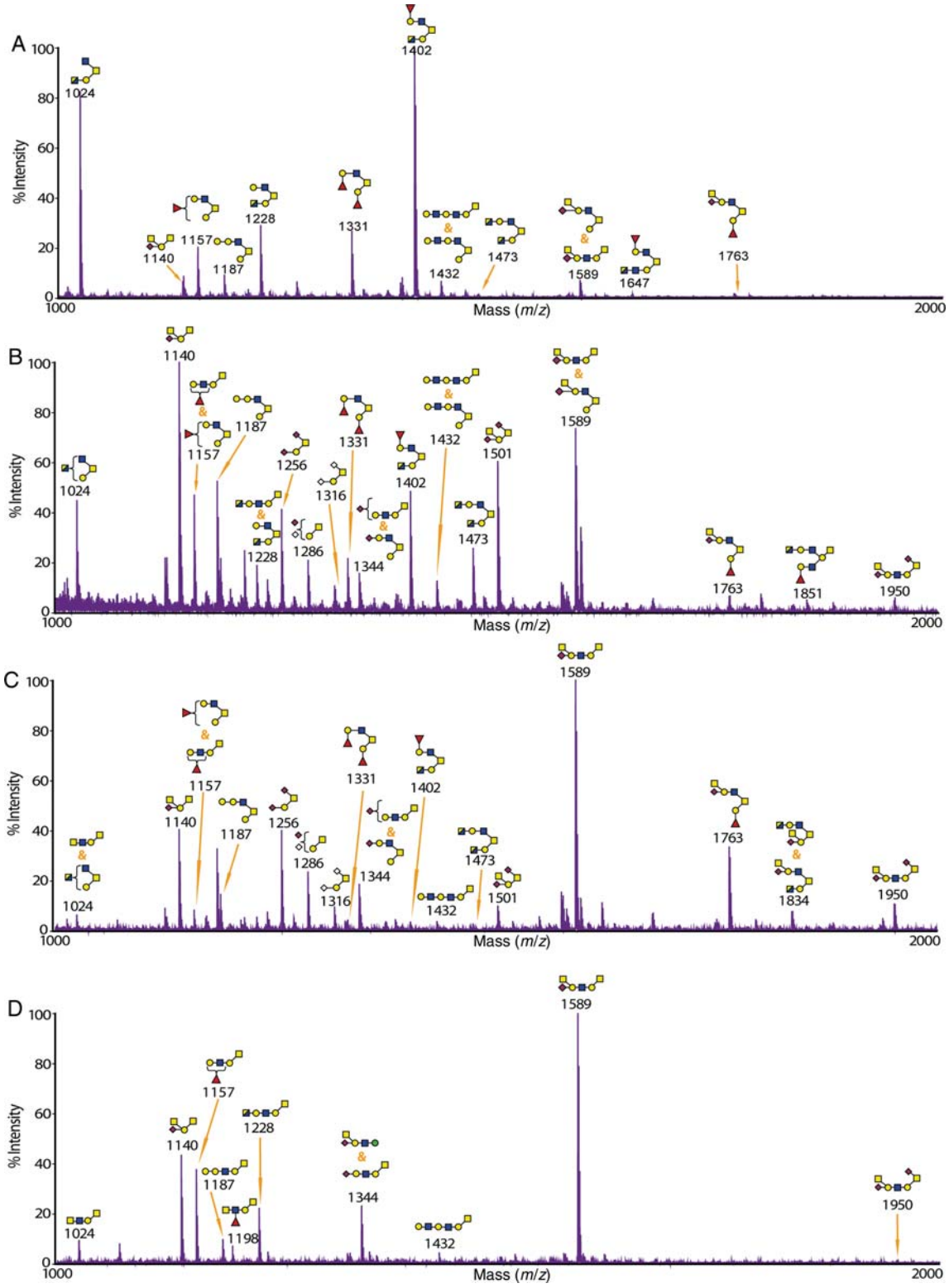

Fig. 4. MALDI-TOF-MS spectra of *O*-glycans from the small intestine of wild-type and knockout mice. The glycomic profiles of reduced and permethylated *O*-glycans $[M + Na]^+$ detected in the small intestine of (**A**) wild-type, (**B**) C2GnT2 knockout, (**C**) C2GnT3 knockout and (**D**) C2GnT triple knockout mice. Cartoon structures assigned were based on mass spectrometric data and knowledge of *O*-glycan biosynthetic pathways for the selected range of *m*/*z* 1000–2000. The full-range MALDI-TOF-MS spectra for each tissue are presented in Supplementary data, Figures S11–S14.

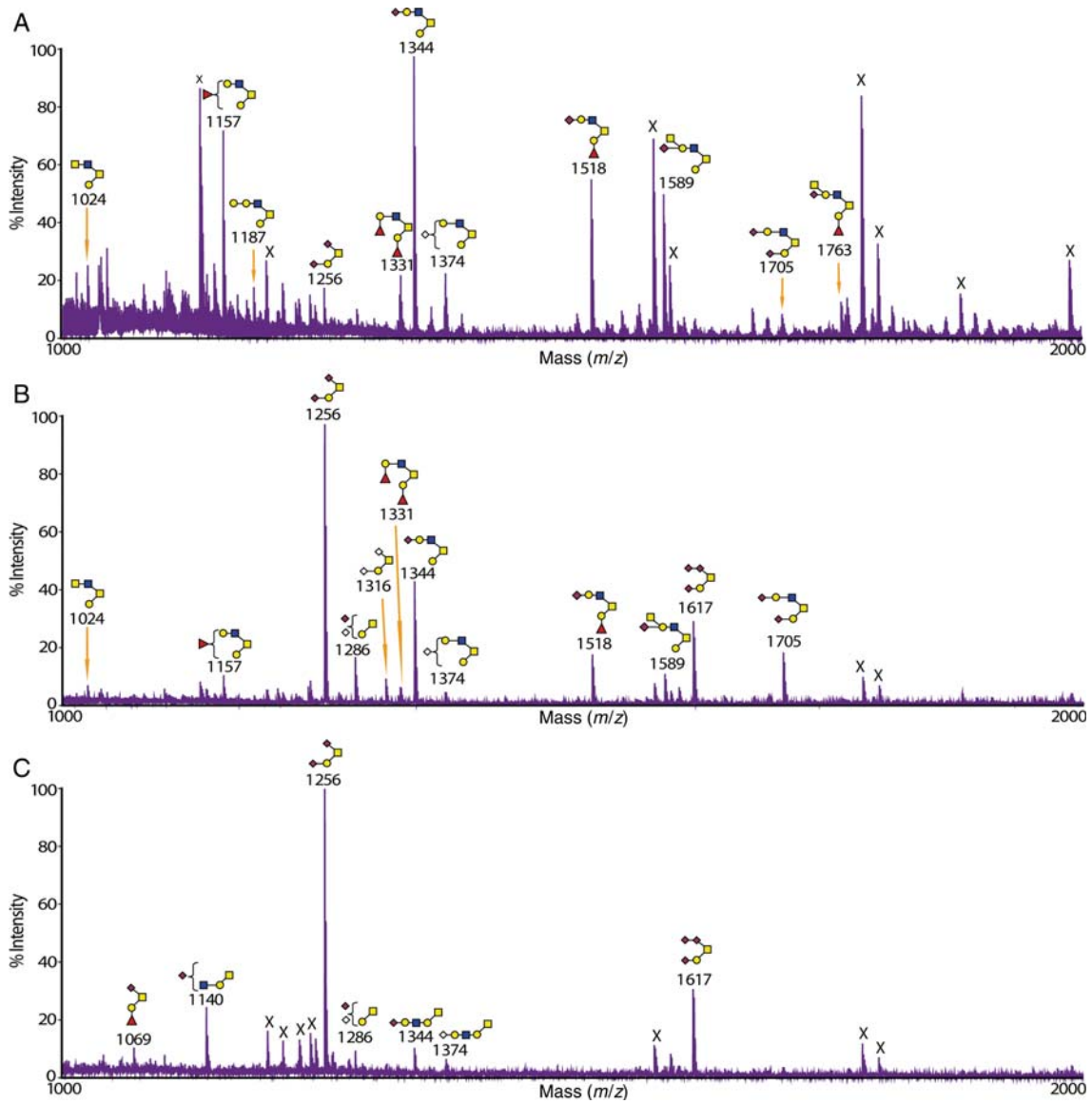

Fig. 5. MALDI-TOF-MS spectra of *O*-glycans from the thyroid/trachea of wild-type and knockout mice. The glycomic profiles of reduced and permethylated *O*-glycans $[M + Na]^+$ detected in the thyroid/trachea of (**A**) wild-type, (**B**) C2GnT3 knockout and (**C**) C2GnT triple knockout mice. Cartoon structures assigned were based on mass spectrometric data and knowledge of *O*-glycan biosynthetic pathways for the selected range of *m*/*z* 1000–2000. X, impurities.

Figure S2A). The *O*-glycans were also highly sialylated with NeuAc or NeuGc, for example, at *m*/*z* 1256 and 1316.

Remarkably, the kidneys from C2GnT2 knockout mice exhibited a significant reduction in the abundance of some of the core 2 *O*-glycans with no concomitant compensation by extended core 1 sequences (Supplementary data, Figure S1B; note loss of *m*/*z* 1402 and higher compared with the wild-type). Thus, only a single glycan structure of the core 1 type (*m*/*z* 1256) was detected in the mass range of *m*/*z* 1000–2000, accompanied by residual core 2 *O*-glycans. The thymus and the thyroid/trachea of C2GnT2 knockout mice were not analyzed due to the absence of any interesting phenotypic findings from these tissues, in addition to the relatively very low expression of C2GnT2 in the wild-type thymus and thyroid/trachea (Stone et al. 2009).

Even though C2GnT3 is believed to play important biological roles in the human thymus (Schwientek et al. 2000), our *O*-glycomic screening has revealed that there were no significant changes, if any, with respect to glycan structures and abundances between the thymus of wild-type and the C2GnT3 knockout mice (Supplementary data, Figure S2B). Similar effects were also observed in the kidneys of C2GnT3 knockout mice (Supplementary data, Figure S1C). In the thyroid/trachea, however, there was a minor disappearance of core 2 structures, and if detected, they were at a much reduced abundance relative to the wild-type, for example, glycan at *m*/*z* 1157, 1589 and 1763, with the latter two being decorated with the Sd^a epitope (Figure 5B).

In the C2GnT triple knockout mice, the thyroid/trachea and the kidneys also exhibit a complete absence of core 2

O-glycans (Figure 5C and Supplementary data, Figure S1D), similar to that seen in other tissues. In the thyroid/trachea of C2GnT triple knockout, there was also a complete absence of glycans bearing the Sd[a] epitope (Figure 5C). Meanwhile in the kidneys, the glycomic analysis revealed a remarkable loss of *O*-glycans with only two structures having simple core 1 type sequences being detected (Supplementary data, Figure S1D). The thymus of C2GnT triple knockout mice was not analyzed.

Determination of N*-acetyllactosamine chain type and branching sites in the stomach and the colon*

Stomach and colon tissues exhibited very varied *O*-glycan structures accompanied by dramatic changes in the knockout tissues. In addition, the MS/MS data provided evidence for a number of potentially biologically important glycan epitopes in these tissues. To put some of these structural assignments on a firmer footing, we were fortunate to have access to a novel MALDI-QIT-TOF mass spectrometer (Ojima et al. 2005), which has been developed for high-accuracy, ultra-high-sensitivity MS/MS/MS analyses. Thus, we performed MS/MS/MS analysis on selected glycan MS/MS fragments that contain linear and branched *N*-acetyllactosamine (LacNAc) chains in order to define backbone linkages and branching sites.

LacNAc chain type 1 consists of the repeating unit Galβ1-3GlcNAcβ1-3, whereas type 2 consists of Galβ1-4GlcNAcβ1-3. As an example of the determination of LacNAc chain type, Figure 6 shows MALDI-QIT-TOF-MS/MS data for the glycan at *m/z* 1780 ($HexNAc_3Hex_3Fuc_2$) of wild-type stomach (Figure 6A), together with MS/MS/MS spectra from collisional activation of the fragments at *m/z* 660 (Figure 6B) and 1143 (Figure 6C). The cross-ring fragments at *m/z* 503 and 586 in Figure 6B unequivocally provide the evidence that the Gal residue is linked to position 4 of GlcNAc. Therefore, this LacNAc unit is confirmed to be type 2. Moreover, the fucose (Fuc) residue was shown to be attached on Gal making this trisaccharide a blood group H type 2 antigen. In addition, enzymatic digestion by using a specific β1,4-galactosidase has shown a major reduction in glycans that are terminated with unmodified Gal in the wild-type stomach compared with the undigested tissue (data not shown), confirming a significant composition of Gal attached to position 4 of GlcNAc in this tissue. This finding is further supported by GC-EI-MS linkage analysis that has shown the existence of 4-linked GlcNAc in the stomach and the colon, whereas 3-linked GlcNAc was not detected in either tissue (data not shown). Taken together, our MS/MS/MS, enzymatic

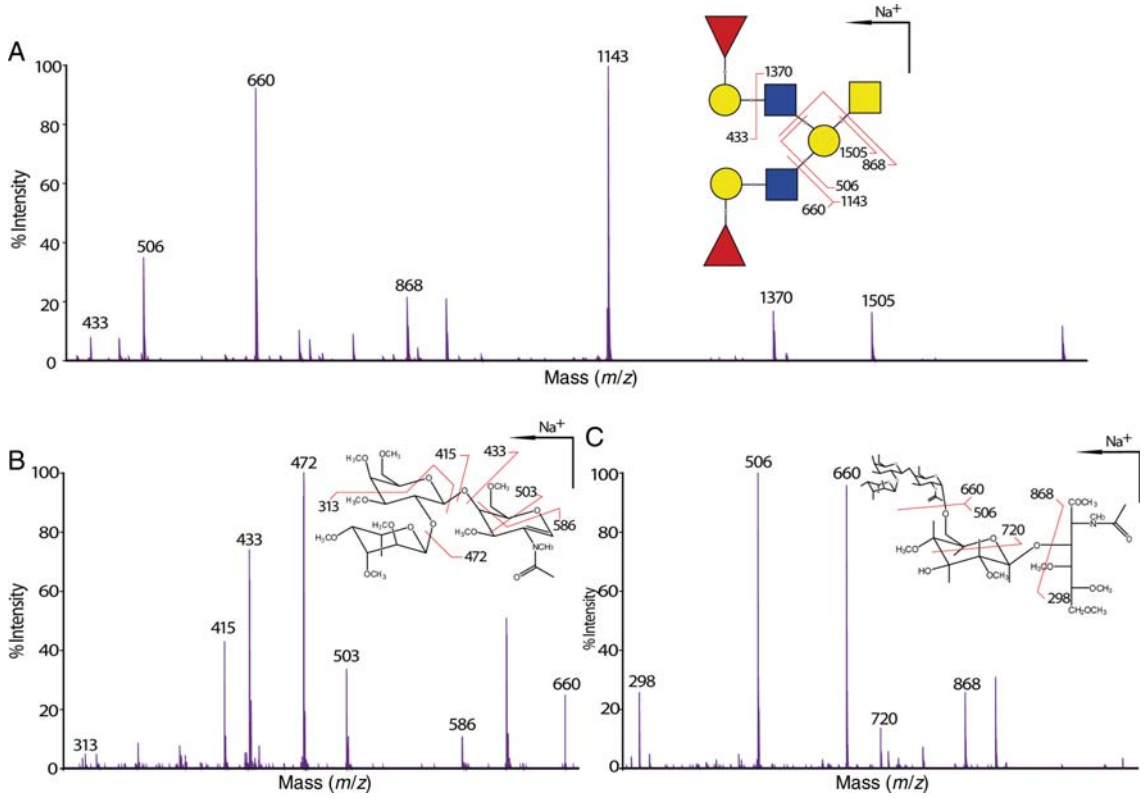

Fig. 6. Determination and verification of LacNAc chain type and I-branch position. (**A**) MALDI-QIT-TOF-MS/MS spectrum of *m/z* 1780 $[M + Na]^+$ from wild-type stomach shows evidence of branching on Gal of the core 1 arm (fragments *m/z* 506 and 1143) and the terminal epitope blood group H antigen on each of the branches (fragments *m/z* 660 and 1370). (**B**) MALDI-QIT-TOF-MS/MS/MS spectrum of the fragment *m/z* 660 from (A) shows evidence for 4-linked GlcNAc (cross-ring fragments at *m/z* 503 and 586) indicating LacNAc unit type 2 as well as a Fuc residue linked on the Gal residue (cross-ring fragment at *m/z* 313) establishing the epitope as H type 2. (**C**) The MALDI-QIT-TOF-MS/MS/MS spectrum of the MS/MS fragment at *m/z* 1143 from (A) has provided evidence for additional branch attaching on the position 6 of the Gal residue of the core 1 arm (cross-ring fragment at *m/z* 720). For simplicity, not all fragments were annotated.

digestion and GC linkage data support the absence of type 1 LacNAc sequences in the stomach and the colon.

MS/MS of the glycan at *m/z* 1780 in the wild-type stomach has proven that the core 1 Gal of this glycan is branched (see annotation in Figure 6A). In fact, this is the only location of the I-branch that we have detected in both the stomach and the colon in this study even when the core 1 antenna is elongated with an additional GlcNAc residue, for example, *m/z* 2617 in the stomach tissues (Supplementary data, Figure S4 and Table SI), which carries one more GlcNAc residue on both the core 1 antenna and the I-branch than *m/z* 1780. MS/MS/MS on the fragment at *m/z* 1143 further confirmed the branched Gal, as well as providing additional verification of the known I-branch linking position (Figure 6C). The cross-ring fragment of *m/z* 720 has provided the evidence of a branching on either position 4 or 6. Additionally, GC-EI-MS linkage analysis has shown the existence of a 3,6-linked Gal residue (data not shown).

Characterization of RM2-like structures in the colon

We have detected an unusual terminal epitope in the *O*-glycan observed at *m/z* 1950 ($HexNAc_3Hex_2NeuAc_2$) in the wild-type and knockout tissues of colon (Figure 2 and Table I). Initial MS/MS fragmentation data from the MALDI-TOF/TOF suggested a sialylated Sd^a epitope ($HexNAc_2Hex_1NeuAc_2$) whose composition is identical to a rare epitope originally found on a glycolipid and called the RM2 antigen (Ito et al. 2001). For further confirmation of this structure, we have performed an additional MS/MS analysis on *m/z* 1950 (Figure 7A) as well as MS/MS/MS analysis on two major MS/MS fragments, namely *m/z* 1108 and 1453 using MALDI-QIT-TOF (Figure 7B and C). Glycosidic and cross-ring fragmentation data of the MS/MS/MS experiment explicitly showed that one of the NeuAc residues was attached to the internal GlcNAc residue rather than the GalNAcitol residue, which is another possible position for sialylation. The latter was detected in the small intestine tissues and the C2GnT triple knockout colon tissues. Overall, these MS/MS/MS data supported the RM2 structural assignment of the initial MS/MS analysis.

Discussion

O-glycomic analyses were performed on mice deficient in C2GnT2, C2GnT3 and all three C2GnT isoenzymes (C2GnT triple knockouts) with wild-type mice as a reference. This work aimed to further clarify the functional properties of each of the isoenzymes in various tissues and to associate structural changes with observed phenotypes of the knockout mice. High-quality MS and MS/MS data were obtained by using a

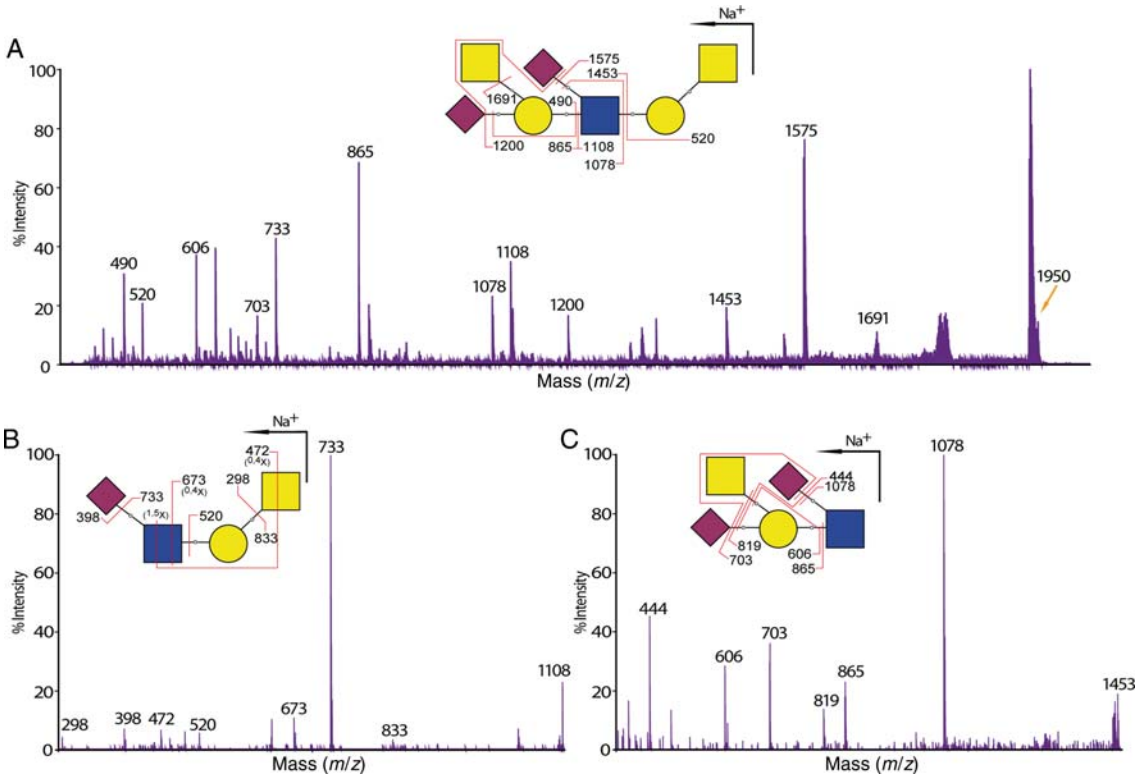

Fig. 7. Structural confirmation of the RM2-like epitope found in the colon tissues. (**A**) MALDI-QIT-TOF-MS/MS spectrum of glycan at *m/z* 1780 $[M+Na]^+$ from wild-type stomach shows evidence for a sialylated Sd^a-terminal epitope. This assignment is further supported by the subsequent MS/MS/MS analysis on the MS/MS fragments of (**B**) *m/z* 1108 and (**C**) *m/z* 1453. Glycosidic and cross-ring fragments at *m/z* 673, 472, 520, 819 and 865 from both MS/MS/MS spectra verified the existence of the Sd^a epitope with additional sialylation on the internal GlcNAc therefore confirming the structural assignment of the MS/MS analysis. For simplicity, not all fragments are annotated.

MALDI-TOF/TOF mass spectrometer in concert with ESI-QTOF, GC-EI and MALDI-QIT-TOF mass spectrometers.

Generally, C2GnT2 knockout mice showed a significant decrease in core 2 *O*-glycans especially in the colon and the stomach compared with the wild-type mice. This was expected as this isoenzyme is highly expressed in these tissues. The glycosylation machinery synthesized more of the extended core 1 *O*-glycans possibly to compensate for the diminishing core 2 *O*-glycans. Position 6 of GalNAcitol of core 1 *O*-glycans was either left unmodified or sialylated. A previous work has characterized core 3 and core 4 *O*-glycans in human intestine (Robbe et al. 2004; Holmen Larsson et al. 2009). In contrast, these core types are hardly expressed in the mouse intestine. Because trace amounts could not be unambiguously determined in the presence of the abundant core 1/2 sequences, addressing possible changes in their abundance as a consequence of loss of C2GnT2 was not feasible.

Branching of the core 1 arm of both core 1 and core 2 *O*-glycans was found to be very abundant especially in the stomach of wild-type mice. C2GnT2 deficiency in mice caused a major reduction and disappearance of glycan branches, therefore demonstrating that C2GnT2 has a strong capability to branch the LacNAc chains specifically on position 6 of the Gal of the core 1 arm. To our knowledge, this analysis is the first to show the I-branching activity of C2GnT2 in vivo using definitive structural analysis. This finding supports previous work that has shown in vitro that human and mouse C2GnT2 have the I-branching capability quite similar to IGnT, but no structural proof was provided (Yeh et al. 1999; Hashimoto et al. 2007). On the basis of in vitro assays, Yeh et al. (1999) suggested that human C2GnT2 possess higher distally acting IGnT activity than centrally acting IGnT activity, although the difference were merely 5%. However, the current finding has shown that centrally attached glycan branches were greatly affected by the loss of C2GnT2 activity. The centrally attached glycan branches specifically on the Gal residue of the core 1 arm was the only type identified in this study, even though the arm was elongated with two LacNAc units. All these data suggest that C2GnT2 acts differently in vivo where it prefers to branch *O*-glycans centrally instead of distally. Similar branching of the Gal residue of the core 1 arm has previously been characterized rigorously on *O*-glycans derived from human Tamm–Horsfall glycoprotein during pregnancy (Easton et al. 2000). Therefore, it is tempting to speculate that C2GnT2's natural substrate is the Gal of GlcNAcβ1-3Galβ1-3GalNAc-Ser/Thr, with or without the core 2 arm attached and elongation on the core 1 arm. The fact that we did not detect other types of branched LacNAc on *O*-glycan is most likely because the IGnT isoenzymes, the only other enzymes known for I-branching activity, are not significantly expressed in a murine gastrointestinal (GI) tract (Twu et al. 2003). We are unable to conclude whether this finding is tissue-specific due to the lack of branched *O*-glycan structures detected in other tissues analyzed.

It was also evident from our data that branched core 1 *O*-glycans were not completely absent in the stomach and the colon of the C2GnT2 single knockout, but were totally lost in the C2GnT triple knockout mice. Therefore, it can be speculated that C2GnT1 and/or C2GnT3 possess a weak I-branching activity and, instead of IGnT, compensated for C2GnT2 I-branching activity in C2GnT2 knockout mice. These results are, however, in contrast with previous immunohistochemical findings on IGnT-deficient mice, which concluded that IGnT is the major enzyme that synthesizes I-branches in the murine stomach (Chen et al. 2005). This discrepancy might be due to the method the previous study applied to detect the reduction in IGnT activity. It is conceivable that the monoclonal antibody against the I antigen that was used could be specific only to I-branches that are attached toward the nonreducing end of a polylactosamine chain (distally), which are supposed to be produced by IGnTs instead of C2GnTs.

We have previously shown that C2GnT2-deficient mice are more susceptible to DSS-induced colitis compared with the wild-type mice (Stone et al. 2009). An et al. (2007) reported that mice with glycosylation changes in their GI tract are more susceptible to colitis. The mechanism of DSS-induced colitis is not clear but destruction of the mucin content is one of the proposed mechanisms (Melgar et al. 2005). It is anticipated that a similar situation is being observed here. The loss of glycan branches (core 2 branches and I-branches) that were observed in the C2GnT2 knockout mice could possibly disrupt the normal glycan structures that protect the underlying proteins in mucin layers.The interrupted conformation of mucins in the GI tract therefore facilitates DSS's destructive action. These changes might be recognized as foreign by the immune system, which is possibly the reason for the increased susceptibility to inflammation which causes colitis. In addition, a direct relationship between immune cells and C2GnT2 has been demonstrated by the upregulation of this isoenzyme by T helper 2 cytokines in human airway mucins (Beum et al. 2005).

C2GnT3 was originally shown by northern blot analysis to be highly expressed in the human thymus and has been implicated to play important roles in T-cell development and lymphocyte trafficking (Schwientek et al. 2000). From our structural *O*-glycomic analysis of the C2GnT3 knockout mice, generally there were no substantial changes on the abundance of core 2 *O*-glycans in any tissues that have been analyzed, albeit a minor reduction was observed in the small intestine and the thyroid/trachea. The lack of any significant changes to *O*-glycan structures and abundances in the thymus of C2GnT3 knockout mice confirms previous qPCR findings that indicated low expression of that isoenzyme in the murine thymus (Stone et al. 2009), as opposed to the human thymus. This indicates that either the other C2GnT isoenzymes can substantially compensate for the loss of C2GnT3 activity or C2GnT3 is not normally responsible for synthesizing the vast majority of core 2 glycans in the murine tissues examined.

It was evident that the loss of C2GnT3 activity caused a slight but reproducible reduction in core 2 *O*-glycans in the thyroid, the thyroxine-producing gland. We have previously shown that in C2GnT3-deficient mice, there is a decrease in the circulating levels of alkaline phosphatase and thyroxine, but the thyroid-stimulating hormone was not affected (Stone et al. 2009). This observation is associated with hypothyroidism but the mechanism is still not fully understood (Fliers

et al. 2006). The major reduction in core 2 *O*-glycans carrying the Sd^a epitope in the C2GnT3-deficient thyroid/trachea is intriguing, supported by the complete loss of Sd^a-terminated glycans in the C2GnT triple-deficient thyroid/trachea, which could illustrate that in the thyroid/trachea, the Sd^a epitope can be synthesized efficiently only on the core 2 arm.We postulate that the population of core 2 *O*-glycans in the thyroid/trachea whose biosynthesis is dominantly controlled by C2GnT3 is somehow necessary in the production of thyroxine. Reduced thyroxine levels will subsequently contribute to the hypothyroidism and the reduction in alkaline phosphatase. Whether the presence of the Sd^a epitope is functionally important in the thyroid remains to be established. The Sd^a epitope has been found on a limited repertoire of interesting glycoproteins in mammals, including human Tamm–Horsfall protein (Serafini-Cessi et al. 1986), the murine zona pellucida (Dell et al. 2003), bovine pregnancy-associated glycoproteins (Klisch et al. 2008) and glycoproteins on murine cytotoxic T-lymphocytes (Smith and Lowe 1994), although no specific function has so far been attributed to this epitope. Glycoproteins from the thyroid that carry these core 2 *O*-glycans would be an important target for further investigations.

Clostridium perfringens and *Helicobacter pylori* are common bacteria that colonize the GI tract. Recently, it has been revealed that *C. perfringens* contains an endo-β-galactosidase that is able to release the disaccharide epitope GlcNAcα1-4Gal from glycoconjugates as part of its pathogenicity (Ashida et al. 2001). It can be interpreted that *C. perfringens* uses this epitope as a binding site to initiate infection. On the other hand, the terminal α1,4-linked GlcNAc residue has been shown to affect the growth of *H. pylori* in the stomach (Kawakubo et al. 2004). Core 2 *O*-glycans capped with this epitope were found to be capable of serving as a natural antibiotic against *H. pylori* infection (Lee et al. 2008). Expression cloning of human α1,4-*N*-acetylglucosaminyltransferase has shown that this epitope is efficiently transferred to core 2 *O*-glycans forming the structure GlcNAcα1-4Galβ1-4GlcNAcβ1-6(GlcNAcα1-4Galβ1-3)GalNAc (Nakayama et al. 1999).We have detected a putative GlcNAcα1-4Gal epitope on the similar core 2 *O*-glycan that is observed at *m/z* 1473 in stomach tissues (Figure 3 and Supplementary data, Table SI). However, the terminal HexNAc residues in stomach have been established to be dominated by β-GlcNAc, using a β-GlcNAc-specific exoglycosidase. Previously,the α-GlcNAc residue has been shown to be expressed specifically on class III mucin in the deeper layer of gastric mucosa (Nakamura et al. 1998); hence, it is very low in abundance and could possibly constitute the residual undigested terminal HexNAc. Intriguingly, this glycan at *m/z* 1473 was well preserved as a core 2 isoform in the C2GnT2 and three single knockout mice and in fact was augmented in the latter tissue, hence illustrating its potential functional importance. Detailed characterization of differences in the glycosylation profile especially in the GI tract is fundamental to better understand host-pathogen interplay (Dell et al. 1999; Magalhães et al. 2010).

From the analysis on C2GnT triple knockout mice, we observed a complete absence of core 2 *O*-glycans in all tissues. Therefore, we propose that there is no other C2GnT isoenzyme in mouse. In addition, we have also noted that due to the major loss of the core 2 antennae and the I-branches on core 1 antennae, several unique glycans that were not originally being synthesized in the wild-type murine tissues have emerged, for instance, the triply fucosylated glycan at *m/z* 1505 in the stomach which is predicted to be a novel structure (Figure 3D and Supplementary data, Table SI). Our MS/MS, linkage analysis and enzymatic digestion data have shown that LacNAc chain type 2 dominated the stomach and the colon; therefore, the immense amount of fucosylated Gal and difucosylated LacNAc terminals are likely to be H type 2 and $Lewis^y$ antigens, respectively.

O-linked mannosyl glycans were first identified in 1969 in yeast and were found to be very abundant in the cell wall (Sentandreu 1969). It was only discovered in the mammalian system 10 years later on a brain proteoglycan (Finne et al. 1979). Subsequently, it has been recognized to constitute 30% of brain *O*-glycans (Chai et al. 1999) and also to be a crucial modification on α-dystroglycan especially in the muscle tissues (Endo 1999). Unexpectedly, *O*-linked mannosyl glycans were upregulated in the stomach of the triple knockout mouse, being barely detected in the wild-type and single knockouts. Cells possibly amplified the addition of complex antennae to *O*-linked mannose in order to replace the diminished core 2 *O*-glycans. Reduced competition for UDP-GlcNAc, which is the donor substrate for both C2GnT and the *O*-mannose elongating enzyme protein-*O*-mannose-β1,2-*N*-acetylglucosaminyltransferase 1 (Takahashi et al. 2001), might explain this observation. To our knowledge, our findings reported here constitute the first structural characterization of *O*-linked mannose in the mucin-rich GI tract. Our linkage analysis has so far provided evidence only for the 2-substituted mannitol residue and not for the branched 2,6-substituted mannitol that has been additionally shown to be present in neural tissues (Yuen et al. 1997). Terminal modification such as sialylation and Lewis antigens have been described on *O*-linked mannosyl glycans (Chiba et al. 1997; Smalheiser et al. 1998). In this study, we have identified multifucosylated components of elongated *O*-linked mannose with up to three Fuc and three LacNAc repeats in the stomach of C2GnT triple knockout mice (*m/z* 1709 and *m/z* 1985, respectively). In addition, a glycan whose composition is consistent with a unique elongated *O*-linked mannose sequence terminated with the Sd^a epitope was detected in the small intestine of C2GnT triple knockout mice. To our knowledge, these modifications of *O*-mannosyl glycans have not been reported elsewhere. It is anticipated that the current findings will open up new avenues for research of *O*-linked mannose.

In contrast to the GI tract, there seems to be no induction of any types of *O*-glycan accompanying the loss of core 2 *O*-glycans in the kidneys of single and triple deficient mice. In the C2GnT2 knockout kidneys, we observed a substantial reduction in some of the core 2 sequences, most notably those with extended core 1 and core 2 antennae (see Supplementary data, Figure S1, glycans at *m/z* 1402 and higher). This was unexpected because Ellies et al. (1998) have previously shown that the kidneys of the C2GnT1 knockout mouse exhibit over 90% reduction in core 2 activity compared with

the wild-type suggesting that the C2GnT1 isoform is responsible for most of the core 2 synthesis in this organ. We consider it likely that C2GnT2 plays an important role in biosynthesis of a portion of the *O*-glycan repertoire in the kidney and that C2GnT1 is not able to compensate for its absence, thereby leading to the disappearance of certain core 2 *O*-glycan sequences. Furthermore, only two *O*-glycan structures of core 1 type were detected in the kidneys of C2GnT triple knockout mice. It is intriguing that the glycosylation system in the kidneys was unable to compensate for the loss of core 2 *O*-glycans by synthesizing other types of *O*-glycans, as has been seen in the stomach and the colon.

Another interesting finding from the murine GI tract is the detection of a sialylated Sd^a terminal sequence ($HexNAc_2Hex_1NeuAc_2$) on the glycan at *m/z* 1950 in the colon of wild-type and knockout mice (Figure 2 and Table I). This structure has been confirmed with MS/MS and is found to share its terminal sequence with the RM2 antigen of glycolipids; therefore, it is designated as the RM2-like antigen. The RM2 antigen was reported as a novel ganglioside in 2001 after being detected by the RM2 antibody (Ito et al. 2001) and is now well recognized as a prostate cancer marker (Saito et al. 2005). To our knowledge, this work is the first to identify the RM2 antigen in glycoproteins. In addition, we also have detected a putative fucosylated version of this glycan at *m/z* 2125 in the colon of wild-type and C2GnT3 knockout mice (Supplementary data, Figures S3 and S5). This very low abundance component remains to be rigorously characterized.

Understanding the functional consequences of the changes to glycan-terminal epitopes and branching observed in the knockout tissues, especially the triple knockouts, will require considerable further work, although clues have already been provided by our published phenotypic studies (Stone et al. 2009). Often, the terminal epitopes are the biologically important part of any particular glycan. Research has shown numerous examples of glycan epitopes serving as messengers between cells of similar or different types including cancer cells and microorganisms (Ashida et al. 2001; Magalhaes et al. 2009; Rydell et al. 2009; Cazet et al. 2010). The type of chain or branch where these antigens reside is not of any less significance in many cases (Mitoma et al. 2003; Muramatsu et al. 2008). Therefore, it would be interesting to challenge these knockout mice with more biological stress and microorganism infection and evaluate the effects of the structural aberrations.

Materials and methods

Animals

Knockout mice were prepared as reported previously (Stone et al. 2009). Tissues harvested include the stomach, colon, small intestine, thyroid/trachea, thymus and kidneys. MS analyses were performed on selective tissues based on the expression levels of C2GnTs in at least duplicates and supplemented by phenotypic data emerging throughout the study.

Glycomic strategy

The overall glycomic strategy employed was similar to earlier methodologies with each step being optimized to improve the recovery and detection of *O*-glycans (Dell 1990; Dell et al. 1994; Sutton-Smith and Dell 2006; Parry et al.)

Tissue homogenization and protein extraction

This procedure has been described previously (Sutton-Smith and Dell 2006). Briefly, tissues were first weighed and then were disrupted on ice by using a homogenizer in the presence of 5 mL homogenization buffer (25 mM Tris, 150 mM NaCl, 5 mM EDTA and 1% CHAPS at pH 7.4). Lysates were then dialyzed against 50 mM ammonium bicarbonate (Ambic; Sigma-Aldrich, UK) buffer at 4°C for 48 h with several buffer changes. This is followed by lyophilization of the tissue lysates.

For stomach, however, glycosphingolipids were separated prior to glycoprotein extraction based on a method that has been described previously (Parry et al. 2007). With assumption that 80% of the tissue weight is water, at least 4 volumes of ice-cold water were added to sample and then homogenized. Then, based on the total water volume in sample, 2.67 volumes of methanol were added and then the samples were mixed vigorously. Next, 1.33 volumes of chloroform were added and followed by vigorous mixing. The samples were then centrifuged (3000 rpm, 10 min). Supernatant that contains glycolipids were carefully discarded. Protein pellets were blown for a few minutes under nitrogen stream to remove excess methanol and chloroform without completely drying the samples. Fifty microliters of 0.6 M Tris buffer was added to each sample and was blown under nitrogen stream without completely drying the samples. Protein pellets were then either reduced and carboxymethylated immediately or kept in −20°C.

Protein reduction and carboxymethylation

Proteins were reduced and carboxymethylated as described previously (Parry et al. 2007). Briefly, lyophilized tissue lysate or protein pellets were reduced by incubation in 0.6 M Tris/4 M guanidine–HCl (Pierce, UK) buffer pH 8.5 containing 2 mg/mL dithiothreitol (Roche, UK) at 50°C for 2 h. This is followed by carboxymethylation in 0.6 M Tris (Sigma-Aldrich, UK) buffer containing 12 mg/mL of iodoacetic acid (Sigma-Aldrich, UK) incubated in the dark at room temperature for 2 h. Carboxymethylation was then terminated by dialysis against 50 mM ambic buffer, pH 8.5, at 4°C for 48 h with several buffer changes, followed by lyophilization.

Cleavage into peptides and glycopeptides

Protein digestion using TPCK-treated, bovine pancreas trypsin (EC 3.4.21.4, Sigma-Aldrich, UK) and purification was performed as described previously (Sutton-Smith and Dell 2006). For each microgram of tissue sample, 1.5 µg of trypsin from a trypsin solution in 50 mM ambic buffer (pH 8.5) was added to the lysates and was incubated at 37°C for 14 h, followed by purification with Oasis HLB extraction cartridges (Waters, UK).

The cartridges were successively conditioned with 5 mL of methanol, 5 mL of 5% (v/v) acetic acid, 5 mL of propan-1-ol and 15 mL of 5% (v/v) acetic acid. The digested samples were then loaded onto the cartridges, washed with 20 mL of

acetic acid (5% v/v) to remove hydrophilic contaminants, and then eluted sequentially with 5 mL of each 20% and 40% propan-1-ol solution in 5% (v/v) acetic acid. The propan-1-ol elutions, which contain glycopeptides and peptides, were concentrated with the Savant SpeedVac (Thermo Fisher Scientific, UK), combined and subsequently lyophilized overnight.

Digestion of N-glycans from glycopeptides

The lyophilized glycopeptide and peptide fractions were dissolved in 200–300 μL of 50 mM ambic buffer (pH 8.4) before adding in a total of 5 U of PNGase F (EC 3.5.1.52, Roche) and incubate at 37°C for 24 h. The samples were then lyophilized overnight and re-dissolved in 200 μL of 5% (v/v) acetic acid for solid-phase extraction with Sep-Pak C_{18} cartridges (Waters, UK) as described for the tryptic digested lysates. The acetic acid fractions, which contain the released *N*-glycans, were lyophilized and later permethylated. The propan-1-ol eluents, which contain *O*-glycopeptides, were combined prior to lyophilization and then ready for release of *O*-glycans.

Release of O-glycans from glycopeptides

Reductive elimination of *O*-glycans was performed as explained previously (Sutton-Smith and Dell 2006). Four hundred microliters of 0.1 M potassium hydroxide (Sigma-Aldrich, UK) containing potassium borohydride (54 mg/mL) (Sigma-Aldrich, UK) was added to dried samples and incubates at 45°C for 14–16 h. The reaction was terminated by adding a few drops of 5% (v/v) acetic acid followed by purification with Dowex 1-X8 desalting column (Sigma-Aldrich, UK).

To prepare the desalting column, a 150 mm Pasteur pipette was fitted with a small piece of glass wool inside it and a piece of silicone tubing at its tapered end and then packed with Dowex beads for each of the sample. The columns were first washed with 15 mL of 5% (v/v) acetic acid. Next, the samples were loaded carefully on the top of the column and then eluted with 7 mL of 5% (v/v) acetic acid. The volume of the eluents was reduced with Savant SpeedVac followed by lyophilization for overnight. Excess borates in the samples were removed by co-evaporating with 10% (v/v) acetic acid in methanol (4 × 0.5 mL) under a stream of nitrogen at room temperature. The purified native *O*-glycans were subsequently permethylated.

Chemical derivatization of O-glycans

Sodium hydroxide (NaOH) permethylation was performed according to an established procedure as described previously (Dell 1990). Briefly, 5–7 NaOH pellets (Sigma-Aldrich, UK) were ground to fine powder and mixed with 2–3 mL anhydrous dimethyl sulfoxide (Romil, UK) before adding to each dried sample. This is followed by the addition of 0.5–0.7 mL of methyl iodide (Alfa Aeser, UK) and vigorous shaking at room temperature for 15 min. Permethylated glycans were extracted with chloroform and then purified by using Sep-Pak C_{18} cartridges.

The cartridges were successively conditioned with methanol (5 mL), water (5 mL), acetonitrile (5 mL) and water (15 mL). Each sample was dissolved in 200 μL of methanol:water (1:1) solution before loading onto the cartridges. The cartridges were washed with 5 mL of water and then eluted sequentially with 3 mL of each 15, 35 and 50% propan-1-ol solution in water. All eluents were then concentrated with a Savant SpeedVac and subsequently lyophilized. Samples were then ready for MS analysis or derivatization for linkage analysis.

Derivatization of glycans for linkage analysis

Partially methylated alditol acetates for GC-EI-MS analysis were prepared from permethylated glycans according to the procedure described previously (Sutton-Smith and Dell 2006). Briefly, samples were first hydrolyzed to partially methylated monosaccharides by incubation in 200 μL of 2 M trifluoroacetic acid (TFA; Romil) at 121°C for 2 h. This is followed by a reducing process with 200 μL of 10 mg/mL $NaBD_4$ in 2 M ammonia solution at room temperature for 2 h. Samples were then acetylated by incubation in 200 μL of acetic anhydride at 100°C for 1 h and then dried under nitrogen stream. The resulting partially methylated alditol acetate monosaccharides were extracted with chloroform the same way as permethylated glycans. The samples were finally dried under nitrogen stream.

MS analysis

MALDI-TOF/TOF-MS and tandem mass spectrometry. MALDI-MS data were acquired by using the 4800 MALDI-TOF/TOF analyzer mass spectrometer (Applied Biosystems) in the positive-ion and reflectron mode by using 2,5-dihydroxibenzoic acid (DHB; Sigma-Aldrich, UK; 20 mg/mL in 70:30 methanol:water) as the matrix. The instrument was calibrated by using peptides from the 4700 Mass Standards kit in (Applied Biosystems, UK) α-cyano-4-hydroxycinnamic acid (CHCA; Sigma-Aldrich, UK; 10 mg/mL in 50:40:10 methanol:water:TFA). MS/MS data were acquired by using the same instrument with the collision energy set at 1 kV. Argon was used as the collision gas with pressure at 3.5×10^{-6} torr.

ESI-QTOF tandem mass spectrometry. ESI-QTOF-MS/MS data were acquired by using the Qstar Pulsar Hybrid System mass spectrometer (Applied Biosystems) in the positive-ion mode and precalibrated with 10–100 fmol/μL of [Glu^1]-fibrinopeptide B (Applied Biosystems, UK) in 5% (v/v) acetonitrile/acetic acid. A few microliters of permethylated samples dissolved in methanol was injected into the instrument. The collision energy used was varied between 30 and 90 eV depending on the size and the nature of the target glycan. The collision gas used was nitrogen with pressure at 5.3×10^{-5} torr.

GC-EI mass spectrometry. The partially methylated alditol acetate samples were reconstituted in a small amount of hexane. Data were acquired by using the Clarus 560 D GC mass spectrometer (Perkin Elmer) fitted with an RTX-5MS column (30 m × 0.25 mm internal diameter; Thames Restek, UK). The samples were injected into the column at 60°C and then the temperature was increased at 8°C/min to 300°C.

MALDI-QIT-TOF-MS and tandem mass spectrometry. Permethylated glycan samples were resuspended in 5 μL of 80% methanol/water. One microliter of sample was then spotted on stainless steel MALDI target and allowed to air-dry. Then, 1 μL of DHB matrix solution (10 mg/mL in 80% methanol/water) was deposited onto the same position and allowed to air-dry. Samples were analyzed by using Axima Resonance MALDI-QIT-TOF mass spectrometer (Shimadzu, UK) in the "mid-850" positive-ion mode. The instrument was calibrated by using peptide standards in CHCA (5 mg/mL in 50/50 acetonitrile/0.1% TFA). Argon was used as the collision-induced dissociation (CID) gas.

Supplementary data

Supplementary data for this article is available online at http://glycob.oxfordjournals.org/.

Funding

The Biotechnology and Biological Sciences Research Council (B19088 and BBF008309 to A.D. and S.M.H.); National Institute of Health (DK48247, HL57345, and CA71932 to J.D.M.).

Acknowledgements

We thank Matthew Openshaw from Shimadzu Biotech, Manchester, UK, for the analyses on Axima Resonance MALDI-QIT-TOF-MS. M.N.I. PhD studentship is sponsored by University Sains Malaysia, Ministry of Higher Education.

Conflict of interest

None declared.

Abbreviations

C2GnT, core 2 β1,6-*N*-acetylglucosaminyltransferase; CHCA, α-cyano-4-hydroxycinnamic acid; DHB, 2,5-dihydroxibenzoic acid; DSS, dextran sodium sulfate; EI, electron impact; ESI, electrospray ionization; Fuc, fucose; Gal, galactose; GalNAc, *N*-acetylgalactosamine; GC, gas chromatography; GI, gastrointestinal; GlcNAc, *N*-acetylglucosamine; HexNAc, *N*-acetylhexosamine; IGnT, I-branching β-1,6-*N*-acetylglucosaminyltrasferase; LacNAc, *N*-acetyllactosamine; MALDI, matrix-assisted laser desorption/ionization; MS, mass spectrometry; MS/MS, tandem mass spectrometry; *m*/*z*, mass over charge ratio; NaOH, sodium hydroxide; NeuAc, *N*-acetylneuraminic acid; NeuGc, *N*-glycolylneuraminic acid; TFA, trifluoroacetic acid; Tn, threonine; TOF, time-of-flight; Q, quadrupole; QIT, quadrupole ion trap.

References

An G, Wei B, Xia B, McDaniel JM, Ju T, Cummings RD, Braun J, Xia L. 2007. Increased susceptibility to colitis and colorectal tumors in mice lacking core 3 derived *O*-glycans. *J Exp Med*. 204(6):1417–1429.

Ashida H, Anderson K, Nakayama J, Maskos K, Chou C-W, Cole RB, Li S-C, Li Y-T. 2001. A novel endo-β-galactosidase from *Clostridium perfringens* that liberates the disaccharide GlcNAcα1-4Gal from glycans specifically expressed in the gastric gland mucous cell-type mucin. *J Biol Chem*. 276(30):28226–28232.

Austin CP, Battey JF, Bradley A, Bucan M, Capecchi M, Collins FS, Dove WF, Duyk G, Dymecki S, Eppig JT, et al. 2004. The knockout mouse project. *Nat Genet*. 36(9):921–924.

Beum PV, Basma H, Bastola DR, Cheng P-W. 2005. Mucin biosynthesis: Upregulation of core 2 β-1,6 *N*-acetylglucosaminyltransferase by retinoic acid and Th2 cytokines in a human airway epithelial cell line. *Am J Physiol Lung Cell Mol Physiol*. 288(1):L116–L124.

Bierhuizen MF. 1992. Expression cloning of a cDNA encoding UDP-GlcNAc:Gal beta 1-3-GalNAc-R (GlcNAc to GalNAc) beta 1-6GlcNAc transferase by gene transfer into CHO cells expressing polyoma large tumor antigen. *Proc Natl Acad Sci USA*. 89(19):9326.

Cazet A, Julien S, Bobowski M, Krzewinski-Recchi M-A, Harduin-Lepers A, Groux-Degroote S, Delannoy P. 2010. Consequences of the expression of sialylated antigens in breast cancer. *Carbohydr Res*. 345(10):1377–1383.

Chai W, Yuen CT, Kogelberg H, Carruthers RA, Margolis RU, Feizi T, Lawson AM. 1999. High prevalence of 2-mono- and 2,6-di-substituted manol-terminating sequences among O-glycans released from brain glycopeptides by reductive alkaline hydrolysis. *Eur J Biochem*. 263 (3):879–888.

Chen G-Y, Muramatsu H, Kondo M, Kurosawa N, Miyake Y, Takeda N, Muramatsu T. 2005. Abnormalities caused by carbohydrate alterations in I β-6-*N*-acetylglucosaminyltransferase-deficient mice. *Mol Cell Biol*. 25 (17):7828–7838.

Chiba A, Matsumura K, Yamada H, Inazu T, Shimizu T, Kusunoki S, Kanazawa I, Kobata A, Endo T. 1997. Structures of sialylated *O*-linked oligosaccharides of bovine peripheral nerve α-dystroglycan. *J Biol Chem*. 272(4):2156–2162.

Dell A. 1990. Preparation and desorption mass spectrometry of permethyl and peracetyl derivatives of oligosaccharides. In: James AM, editor. *Methods in Enzymology*, vol. 193. San Diego, USA: Academic Press. p. 647–660.

Dell A, Chalabi S, Easton RL, Haslam SM, Sutton-Smith M, Patankar MS, Lattanzio F, Panico M, Morris HR, Clark GF. 2003. Murine and human zona pellucida 3 derived from mouse eggs express identical O-glycans. *Proc Natl Acad Sci USA*. 100(26):15631–15636.

Dell A, Haslam SM, Morris HR, Khoo K-H. 1999. Immunogenic glycoconjugates implicated in parasitic nematode diseases. *Biochim Biophys ActaMol Basis Dis*. 1455(2–3):353–362.

Dell A, Reason AJ, Khoo K-H, Panico M, McDowell RA, Morris HR, William JL, Gerald WH. 1994. Mass spectrometry of carbohydrate-containing biopolymers. In: Lennarz WJ, Har GW, editors. *Methods in Enzymology*, vol. 230. San Diego, USA: Academic Press. p. 108–132.

Easton RL, Patankar MS, Clark GF, Morris HR, Dell A. 2000. Pregnancy-associated changes in the glycosylation of Tamm-Horsfall glycoprotein. *J Biol Chem*. 275(29):21928–21938.

Ellies LG, Tsuboi S, Petryniak B, Lowe JB, Fukuda M, Marth JD. 1998. Core 2 oligosaccharide biosynthesis distinguishes between selectin ligands essential for leukocyte homing and inflammation. *Immunity*. 9(6):881–890.

Endo T. 1999. *O*-mannosyl glycans in mammals. *Biochim Biophys Acta*. 1473 (1):237–246.

Finne J, Krusius T, Margolis RK, Margolis RU. 1979. Novel mannitol-containing oligosaccharides obtained by mild alkaline borohydride treatment of a chondroitin sulfate proteoglycan from brain. *J Biol Chem*. 254 (20):10295–10300.

Fliers E, Unmehopa UA, Alkemade A. 2006. Functional neuroanatomy of thyroid hormone feedback in the human hypothalamus and pituitary gland. *Mol Cell Endocrinol*. 251(1-2):1–8.

Gauguet J-M, Rosen SD, Marth JD, von Andrian UH. 2004. Core 2 branching {beta}1,6-*N*-acetylglucosaminyltransferase and high endothelial cell *N*-acetylglucosamine-6-sulfotransferase exert differential control over B- and T-lymphocyte homing to peripheral lymph nodes. *Blood*. 104 (13):4104–4112.

Hashimoto M, Tan S, Mori N, Cheng H, Cheng P-W. 2007. Mucin biosynthesis: Molecular cloning and expression of mouse mucus-type core 2 β1,6 *N*-acetylglucosaminyltransferase. *Glycobiology*. 17(9):994–1006.

Hiraoka N, Kawashima H, Petryniak B, Nakayama J, Mitoma J, Marth JD, Lowe JB, Fukuda M. 2004. Core 2 branching β1,6-*N*-acetylglucosaminyltransferase and high endothelial venule-restricted sulfotransferase collaboratively control lymphocyte homing. *J Biol Chem*. 279(4):3058–3067.

Holmen Larsson JM, Karlsson H, Sjovall H, Hansson GC. 2009. A complex, but uniform O-glycosylation of the human MUC2 mucin from colonic biopsies analyzed by nanoLC/MSn. *Glycobiology*. 19(7):756–766.

Ito A, Levery SB, Saito S, Satoh M, Hakomori S-I. 2001. A novel ganglioside isolated from renal cell carcinoma. *J Biol Chem*. 276 (20):16695–16703.

Kawakubo M, Ito Y, Okimura Y, Kobayashi M, Sakura K, Kasama S, Fukuda MN, Fukuda M, Katsuyama T, Nakayama J. 2004. Natural antibiotic function of a human gastric mucin against *Helicobacter pylori* infection. *Science*. 305(5686):1003–1006.

Kikuchi J, Shinohara H, Nonomura C, Ando H, Takaku S, Nojiri H, Nakamura M. 2005. Not core 2 β1,6-*N*-acetylglucosaminyltransferase-2 or -3 but -1 regulates sialyl-Lewis x expression in human precursor B cells. *Glycobiology*. 15(3):271–280.

Klisch K, Jeanrond E, Pang P-C, Pich A, Schuler G, Dantzer V, Kowalewski MP, Dell A. 2008. A tetraantennary glycan with bisecting *N*-acetylglucosamine and the Sd^a antigen is the predominant *N*-glycan on bovine pregnancy-associated glycoproteins. *Glycobiology*. 18(1):42–52.

Lee H, Hoshino H, Wang P, Ito Y, Kobayashi M, Nakayama J, Seeberger PH, Fukuda M. 2008. α1,4GlcNAc-capped mucin-type *O*-glycan inhibits cholesterol α-glucosyltransferase from *Helicobacter pylori* and suppresses *H. pylori* growth. *Glycobiology*. 18(7):549–558.

Magalhaes A, Gomes J, Ismail MN, Haslam SM, Mendes N, Osorio H, David L, Le Pendu J, Haas R, Dell A, et al. 2009. Fut2-null mice display an altered glycosylation profile and impaired BabA-mediated *Helicobacter pylori* adhesion to gastric mucosa. *Glycobiology*. 19(12):1525–1536.

Magalhães A, Ismail MN, Reis CA. 2010. Sweet receptors mediate the adhesion of the gastric pathogen *Helicobacter pylori*: Glycoproteomic strategies. *Expert Rev Proteomics*. 7(3):307–310.

Melgar S, Karlsson A, Michaelsson E. 2005. Acute colitis induced by dextran sulfate sodium progresses to chronicity in C57BL/6 but not in BALB/c mice: Correlation between symptoms and inflammation. *Am J Physiol Gastrointest Liver Physiol*. 288(6):G1328–G1338.

Mitoma J, Petryniak B, Hiraoka N, Yeh J-C, Lowe JB, Fukuda M. 2003. Extended core 1 and core 2 branched *O*-glycans differentially modulate sialyl Lewis x-type L-selectin ligand activity. *J Biol Chem*. 278 (11):9953–9961.

Muramatsu H, Kusano T, Sato M, Oda Y, Kobori K, Muramatsu T. 2008. Embryonic stem cells deficient in I β1,6-*N*-acetylglucosaminyltransferase exhibit reduced expression of embryoglycan and the loss of a Lewis X antigen, 4C9. *Glycobiology*. 18(3):242–249.

Nakamura N, Ota H, Katsuyama T, Akamatsu T, Ishihara K, Kurihara M, Hotta K. 1998. Histochemical reactivity of normal, metaplastic, and neoplastic tissues to α-linked *N*-acetylglucosamine residue-specific monoclonal antibody HIK1083. *J Histochem Cytochem*. 46(7):793–802.

Nakayama J, Yeh J-C, Misra AK, Ito S, Katsuyama T, Fukuda M. 1999. Expression cloning of a human α1,4-*N*-acetylglucosaminyltransferase that forms GlcNAcα1→4Galβ→R, a glycan specifically expressed in the gastric gland mucous cell-type mucin. *Proc Natl Acad Sci USA*. 96 (16):8991–8996.

Ojima N, Masuda K, Tanaka K, Nishimura O. 2005. Analysis of neutral oligosaccharides for structural characterization by matrix-assisted laser desorption/ionization quadrupole ion trap time-of-flight mass spectrometry. *J Mass Spectrom*. 40(3):380–388.

Parry S, Ledger V, Tissot B, Haslam SM, Scott J, Morris HR, Dell A. 2007. Integrated mass spectrometric strategy for characterizing the glycans from glycosphingolipids and glycoproteins: Direct identification of sialyl Le^x in mice. *Glycobiology*. 17(6):646–654.

Robbe C, Capon C, Coddeville B, Michalski J-C. 2004. Structural diversity and specific distribution of O-glycans in normal human mucins along the intestinal tract. *Biochem J*. 384(2):307–316.

Rydell GE, Nilsson J, Rodriguez-Diaz J, Ruvoen-Clouet N, Svensson L, Le Pendu J, Larson G. 2009. Human noroviruses recognize sialyl Lewis x neoglycoprotein. *Glycobiology*. 19(3):309–320.

Saito S, Egawa S, Endoh M, Ueno S, Ito A, Numahata K, Satoh M, Kuwao S, Baba S, Hakomori S, et al. 2005. RM2 antigen (beta1,4-GalNAc-disialyl-Lc4) as a new marker for prostate cancer. *Int J Cancer*. 115 (1):105–113.

Schwientek T, Yeh J-C, Levery SB, Keck B, Merkx G, van Kessel AG, Fukuda M, Clausen H. 2000. Control of O-glycan branch formation. Molecular cloning and characterisation of a novel thymus-associated core 2 beta 1,6-N-acetylglucosaminyltransferase. *J Biol Chem*. 275 (15):11106–11113.

Sentandreu R. 1969. Yeast cell-wall synthesis. *Biochem J*. 115(2):231.

Serafini-Cessi F, Dall'Olio F, Malagolini N. 1986. Characterization of *N*-acetyl-[beta]-D-galactosaminyl-transferase from guinea-pig kidney involved in the biosynthesis of Sda antigen associated with Tamm-Horsfall glycoprotein. *Carbohydr Res*. 151:65–76.

Smalheiser NR, Haslam SM, Sutton-Smith M, Morris HR, Dell A. 1998. Structural analysis of sequences *O*-linked to mannose reveals a novel Lewis X structure in cranin (dystroglycan) purified from sheep brain. *J Biol Chem*. 273(37):23698–23703.

Smith PL, Lowe JB. 1994. Molecular cloning of a murine N-acetylgalactosamine transferase cDNA that determines expression of the T lymphocyte-specific CT oligosaccharide differentiation antigen. *J Biol Chem*. 269:15162–15171.

Stone EL, Ismail MN, Lee SH, Luu Y, Ramirez K, Haslam SM, Ho SB, Dell A, Fukuda M, Marth JD. 2009. Glycosyltransferase function in core 2-type protein O glycosylation. *Mol Cell Biol*. 29 (13):3770–3782.

Sutton-Smith M, Dell A. 2006. Analysis of carbohydrates/glycoproteins by mass spectrometry. In: Celis J, editor. *Cell Biology: A Laboratory Handbook*. San Diego (CA): Academic Press. p. 415–425.

Takahashi S, Sasaki T, Manya H, Chiba Y, Yoshida A, Mizuno M, Ishida H-K, Ito F, Inazu T, Kotani N, et al. 2001. A new beta-1,2-N-acetylglucosaminyltransferase that may play a role in the biosynthesis of mammalian O-mannosyl glycans. *Glycobiology*. 11(1):37–45.

Tian E, Ten Hagen K. 2009. Recent insights into the biological roles of mucin-type O-glycosylation. *Glycoconj J*. 26(3):325–334.

Twu YC, Chou ML, Yu LC. 2003. The molecular genetics of the mouse I beta-1,6-N-acetylglucosaminyltransferase locus. *Biochem Biophys Res Commun*. 303(3):868–876.

Yeh J-C, Ong E, Fukuda M. 1999. Molecular cloning and expression of a novel beta -1,6-N-acetylglucosaminyltransferase that forms core 2, core 4, and I branches. *J Biol Chem*. 274(5):3215–3221.

Yuen CT, Chai W, Loveless RW, Lawson AM, Margolis RU, Feizi T. 1997. Brain contains HNK-1 immunoreactive O-glycans of the sulfoglucuronyl lactosamine series that terminate in 2-linked or 2,6-linked hexose (mannose). *J Biol Chem*. 272(14):8924–8931.